ARTICLE NO. 79-0936R

J80-104

30018
50002

Nonlinear Stress-Strain Law for Metallic Meshes

S. Tang,* R. Boyle,† J. Whiteside,‡ and R. Anderson§
Grumman Aerospace Corporation, Bethpage, N.Y.

A two-dimensional, orthotropic, nonlinear elastic stress-strain law is proposed herein for gold-coated tricot metallic mesh material of diamond-weave pattern. This constitutive relation accommodates the geometrically nonlinear behavior due to the large displacement of the diamond-shaped cell as well as the nonlinear behavior due to its woven configuration. Comparison with experimental data showed that the proposed constitutive law provides a reasonably good description of the stress-strain behavior of this material.

Introduction

BECAUSE of their high strength and lightweight properties, the use of flexible knitted mesh materials in current and future space based antennas is increasing.[1-5] Compared to other proposed antenna materials, such as perforated sheets, fibrous Mylar, or weaves, a knit has superior mechanical durability and stability. In addition to its low in-plane stiffness, the knitted material allows the mesh to be prestretched and, therefore, wrinkles and sensitivity to thermal distortion are minimized.

There are many varieties of knit patterns of mesh materials. The ones that have been considered for antenna construction include the diamond tricot, hexagonal tulle, square net raschel, single-bar tricot, and marquisette knit.[3] The single-bar tricot is considered unsuitable because it lacks non-run characteristics. The square net raschel is good only for low frequency antennas because of its large mesh openings. The marquisette exhibits unwanted strong polarization. The diamond tricot has a symmetric pattern with an equal number of yarns in both directions to avoid directional rf polarizations. The tulle is almost free of polarization. Both of these knits have low mass/area ratio.

In order to predict the load and deflection distribution of a large space antenna made of mesh material, by either the finite element method or other analytical means, it is desirable to have an analytical constitutive expression. An existing stress-strain law for knitted fabric,[6] which is for single yarn with simple one-loop geometry, cannot be used for the knitted mesh considered here because the meshes have multiple yarns and the knitted mesh configuration is much more complex. Therefore, this article attempts to define the stress-strain relation of a diamond tricot mesh material both experimentally and theoretically. Based on observation, an engineering approach is adopted to form a two-dimensional, orthotropic, nonlinear elastic stress-strain law. The theoretical prediction is then compared to the experimental data. A similar approach may be used to develop the stress-strain relations of the hexagonal tulle.

Presented as Paper 79-0936 at the AIAA/NASA Conference on Advanced Technology for Future Space Systems, Hampton, Va., May 8-11, 1979; submitted June 14, 1979; revision received Oct. 5, 1979.

Index categories: Materials, Properties of; Satellite Communication Systems (including Terrestrial Stations).

*Senior Engineer, Advanced Composites Group, Structural Mechanics Section.
†Project Engineer, Structural Design Section.
‡Applied Mechanics Lab. Head, Research Dept.
§Project Engineer, Advanced Space System.

Theoretical Model

Tests show that the load-displacement curves of a mesh material are highly nonlinear. Diamond tricot in particular exhibits bidirectional nonlinear elastic behavior. Examination shows that the nonlinear behavior of the diamond tricot is the result of two effects. One part comes from the large displacements of the diamond-shaped cell acting as a four-bar linkage. The second effect stems from the knitted pattern of the material. The multiple strands of metal-coated yarn are looped around each other such that when in-plane loading is applied the metal wire is subjected to stretching in the straight portion, as well as bending in the coiled portion. It is believed that the uncoiling contributes to the nonlinear behavior.

To account for the large displacement of a tricot cell, it is represented by a diamond-shaped four-bar linkage as shown in Fig. 1. Each bar has length L and is pin-connected at its end. The applied in-plane tensile loads F_1 and F_2 are related to the angle ϕ in the following way:

$$F_2/F_1 = \tan\phi \tag{1}$$

In textile engineering, the two principal directions 1 and 2 of the fabric are called the wale and course directions, respectively. The coordinate origin is chosen at the center of the diamond cell. By symmetry, the displacements of the four end points are restricted to the vertical or horizontal axis. The relation between two end points of a bar in the first quadrant is given by

$$y/x = \tan\phi \tag{2}$$

Combining Eqs. (1) and (2), we have

$$F_2/F_1 = y/x \tag{3}$$

By eliminating y through the geometric relation $y^2 = L^2 - x^2$, Eq. (3) becomes

$$F_2/F_1 = (L^2 - x^2/x) \tag{4}$$

Squaring both sides of Eq. (4) and rearranging the terms, the position of one of the horizontal end points is:

$$x = \frac{(F_1/F_2)L}{(1+F_1^2/F_2^2)^{1/2}}, \quad F_2 > 0 \tag{5}$$

Similarly, the position of one of the vertical end points is

$$y = \frac{(F_2/F_1)L}{(1+F_2^2/F_1^2)^{1/2}}, \quad F_1 > 0 \tag{6}$$

A plot of X/L vs F_1/F_2 is shown in Fig. 2. Figure 2 shows that the displacement X/L vs the load F_1/F_2 is highly nonlinear.

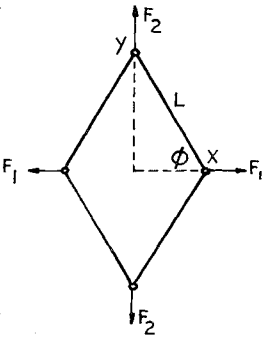

Fig. 1 Schematic representation of a diamond cell.

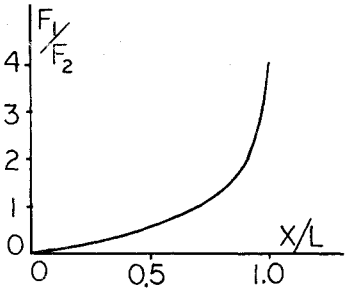

Fig. 2 Geometrically nonlinear behavior of a diamond cell.

This portion of nonlinear behavior is derived from geometric and force balance considerations. No elasticity of the material has yet been taken into account.

To account for the other portion of nonlinear behavior, it is assumed that the uniaxial stress-strain relation obeys a power law[7]:

$$N=K\epsilon^n \quad n>1 \tag{7}$$

where K and n are material constants. A two-dimensional "effective stress" for orthotropic materials is defined as[8,9]

$$N_e=(C_1^2N_1^2+C_2^2N_2^2-C_1C_2N_1N_2+3C_3N_{12}^2)^{1/2} \tag{8}$$

Here N_1 and N_2 are the loads per unit length in the principal directions, wale and course, of the mesh. C_1, C_2 and C_3 are dimensionless constants to be determined experimentally. When $C_1=C_2=C_3=1$, Eq. (8) reduces to the effective stress of an isotropic material.[7] Furthermore, an elastic potential W is assumed to exist:

$$W=N_{ij}\epsilon_{ij} \tag{9}$$

It depends on the scalar effective stress such that

$$\epsilon_{ij}=\frac{dW}{dN_e}\frac{\partial N_e}{\partial N_{ij}} \tag{10}$$

With the requirement that the effective stress N_e and the effective strain ϵ_e be related by the power law

$$N_e=K\epsilon_e^n \quad n>1 \tag{11}$$

the stress-strain relations with respect to the material's natural axes are as follows[7,8]:

$$\epsilon_{11}=\left(\frac{N_e}{K}\right)^{(1-n)/n}\left[\frac{C_1^2N_1}{K}-\frac{C_1C_2N_2}{2K}\right]GF_1$$

$$\epsilon_{22}=\left(\frac{N_e}{K}\right)^{(1-n)/n}\left[\frac{-C_1C_2N_1}{2K}+\frac{C_2^2N_2}{K}\right]GF_2$$

$$\epsilon_{12}=\left(\frac{N_e}{K}\right)^{(1-n)/n}\frac{3C_3N_{12}}{K} \tag{12}$$

Here GF_1 and GF_2 are the geometrical factors from Eqs. (5) and (6):

$$GF_1=\frac{N_1/N_2}{(1+N_1^2/N_2^2)^{1/2}}, \quad N_2>0$$

$$GF_2=\frac{N_2/N_1}{(1+N_2^2/N_1^2)^{1/2}}, \quad N_1>0 \tag{13}$$

It is known that the mesh material does not resist compressive load; it takes only in-plane tensile load and shear load. There are five parameters in Eqs. (12)—n, K, C_1, C_2 and C_3—and they must be determined from the test data.

It should be observed that the power index may also be made as directional constants n_1 and n_2 (Ref. 10). Then the strain-stress law will be more complicated. For a given stress ratio, the strains in the two directions 1, 2 are different, but the curvature of the two curves are the same. Therefore, in this case $n_1=n_2=n$ is adequate to describe the behavior of the mesh material.

When the wale and course directions 1, 2 are not coincident with the loading or reference axes for the mesh x, y, the constitutive relation can be derived by a second order tensor transformation.[11] If we let

$$S_{11}=C_1^2/K, \quad S_{12}=-C_1C_2/2K, \quad S_{22}=C_2^2/K$$

$$S_{66}=3C_3/K, \quad fe=(N_e/K)^{(1-n)/n} \tag{14}$$

Eqs. (12) may be rewritten as

$$\epsilon_{11}=fe(S_{11}N_1+S_{12}N_2)GF_1$$

$$\epsilon_{22}=fe(S_{12}N_1+S_{22}N_2)GF_2$$

$$\epsilon_{12}=feS_{66}N_{12} \tag{15}$$

where the S_{ij} are the compliance parameters.

If the 1, 2 axes are rotated a $+\theta$ from the loading axes x, y, then the strain-stress relations referred to the loading axes are

$$\epsilon_x=fe(\bar{S}_{11}Nx+\bar{S}_{12}Ny+\bar{S}_{16}Nxy)GFx$$

$$\epsilon_y=fe(\bar{S}_{12}Nx+\bar{S}_{22}Ny+\bar{S}_{26}Nxy)GFy$$

$$\epsilon_{xy}=fe(S_{16}Nx+S_{26}Ny+S_{66}Nxy) \tag{16}$$

Since N_e is a scalar and hence does not change with the rotation of axes, the geometrical factors may be derived similarly:

$$GF_x=\frac{(N_1+|N_{12}|)/(N_2+|N_{12}|)}{\left[1+\left(\frac{N_1+|N_{12}|}{N_2+|N_{12}|}\right)^2\right]^{1/2}}$$

$$GF_y=\frac{(N_2+|N_{12}|)/(N_1+|N_{12}|)}{\left[1+\left(\frac{N_2+|N_{12}|}{N_1+|N_{12}|}\right)^2\right]^{1/2}} \tag{17}$$

and the $\bar{S}_{ij}$ are defined as follows[11]

$$\bar{S}_{11}=S_{11}\cos^4\theta+2(S_{12}+2S_{66})\sin^2\theta\cos^2\theta+S_{22}\sin^4\theta$$

$$\bar{S}_{22}=S_{11}\sin^4\theta+2(S_{12}+2S_{66})\sin^2\theta\cos^2\theta+S_{22}\cos^4\theta$$

$$\bar{S}_{12}=(S_{11}+S_{22}-4S_{66})\sin^2\theta\cos^2\theta+S_{12}(\sin^4\theta+\cos^4\theta)$$

$$\bar{S}_{66}=(S_{11}+S_{22}-2S_{12}-2S_{66})\sin^2\theta\cos^2\theta$$

$$+S_{66}(\sin^4\theta+\cos^4\theta)$$

$$\bar{S}_{16} = (S_{11} - S_{12} - 2S_{66})\sin\theta\cos^3\theta + (S_{12} - S_{22} + 2S_{66})\sin^3\theta\cos\theta$$

$$\bar{S}_{26} = (S_{11} - S_{12} - 2S_{66})\sin^3\theta\cos\theta + (S_{12} - S_{22} + 2S_{66})\sin\theta\cos^3\theta \quad (18)$$

The "effective elastic moduli" E_1 and E_2 in the principal directions and the in-plane "effective shear modulus" G_{12} are defined as

$$E_1 = \frac{\partial N_1}{\partial \epsilon_{11}}, \quad E_2 = \frac{\partial N_2}{\partial \epsilon_{22}}, \quad G_{12} = \frac{\partial N_{12}}{\partial \epsilon_{12}} \quad (19)$$

and can be computed from the following formulas:

$$E_1 = \left(\frac{N_e}{K}\right)^{(n-1)/n}(1+N_1^2/N_2^2)^{1/2}\left[2S_{11}N_1/N_2 + S_{12} - \frac{S_{11}N_1^3/N_2^3 + S_{12}N_1^2/N_2^2}{1+N_1^2/N_2^2} - \left(\frac{n-1}{n}\right)\left(C_1^2N_1 - \frac{C_1C_2}{2}N_2\right) \times (S_{11}N_1^2/N_2 + S_{12}N_1)/N_e^2\right]^{-1} \quad (20)$$

$$E_2 = \left(\frac{N_e}{K}\right)^{(n-1)/n}(1+N_2^2/N_1^2)^{1/2}\left[2S_{22}N_2/N_1 + S_{12} - \frac{S_{22}N_2^3/N_1^3 + S_{12}N_2^2/N_1^2}{1+N_2^2/N_1^2} - \left(\frac{n-1}{n}\right)\left(C_2^2N_2 - \frac{C_1C_2}{2}N_1\right) \times (S_{22}N_2^2/N_1 + S_{12}N_2)/N_e^2\right]^{-1} \quad (21)$$

$$G_{12} = \left(\frac{N_e}{K}\right)^{(n-1)/n}\Big/S_{66}(1 - 3C_3N_{12}^2/N_e^2) \quad (22)$$

The "effective Poisson's ratios" ν_{12} and ν_{21} are defined as follows:

$$\nu_{12} = -\epsilon_{22}/\epsilon_{11}, \quad \nu_{21} = \nu_{12}E_2/E_1 \quad (23)$$

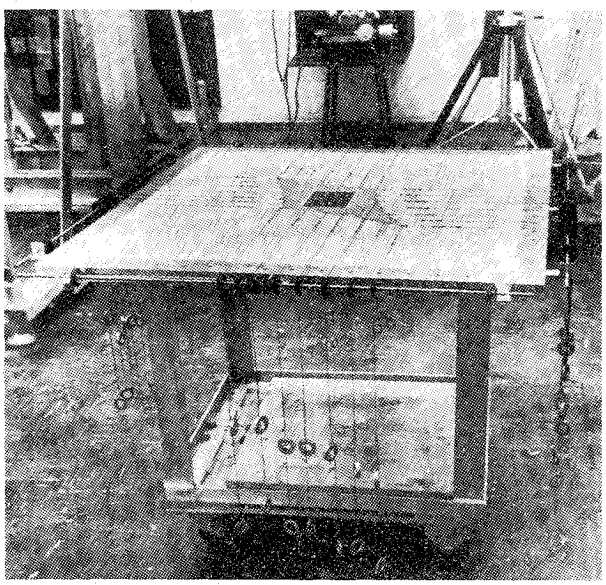

Fig. 3 Experimental equipment.

Table 1 Molybdenum and nichrome wire tricot knitted meshes

Part no.	Material	Wire diam no. fil	Knit gauge	Gold
1	Nichrome	0.0007/7 Fil	32	Unplated
2	Nichrome	0.0007/5 Fil	28	Unplated
3	Nichrome	0.0007/5 Fil	14	Unplated
4	Nichrome	0.0007/7 Fil	28	Plated
5	Moly	0.0015/Mono	20	Plated
6	Moly	0.0012/Mono	28	Plated
7	Nichrome	0.0007/5 Fil	28	Plated

From Eqs. (15) we have

$$\nu_{12} = -(S_{12}N_1 + S_{22}N_2)GF_2/(S_{11}N_1 + S_{12}N_2)GF_1 \quad (24)$$

Together, we have an "effective stiffness matrix Q," such that $\{N\} = [Q]\{\epsilon\}$, with

$$[Q] = \begin{bmatrix} Q_{11} & Q_{12} & 0 \\ Q_{12} & Q_{22} & 0 \\ 0 & 0 & Q_{66} \end{bmatrix} \quad (25)$$

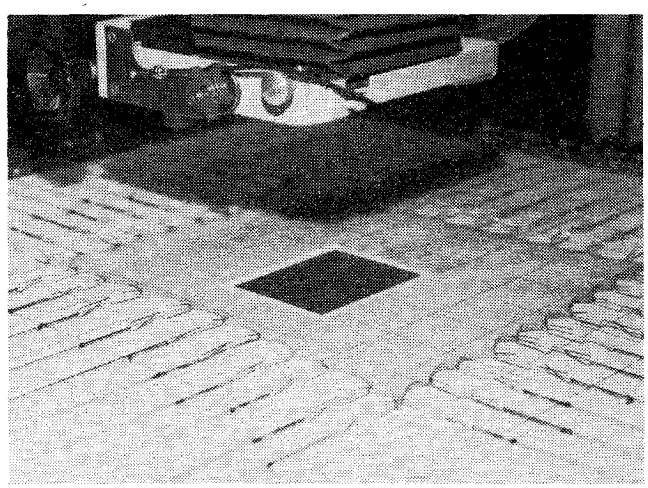

Fig. 4 Loaded in principal directions.

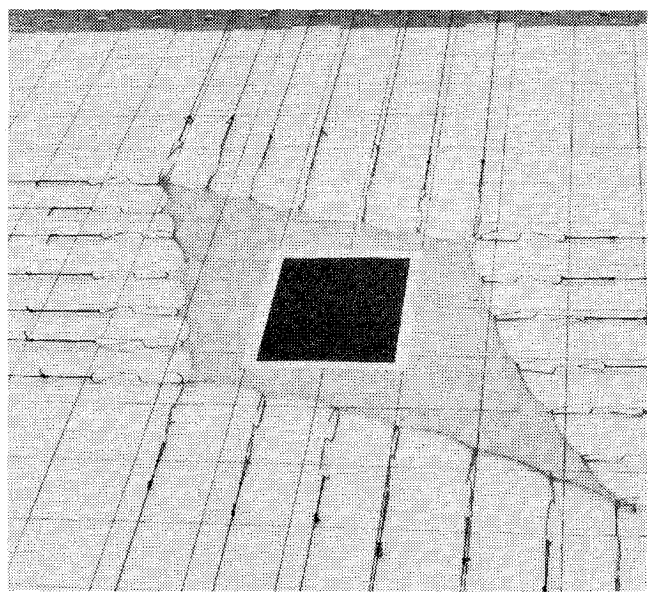

Fig. 5 Loaded off principal directions.

where

$$Q_{11}=E_1/(1-\nu_{12}\nu_{21}),\quad Q_{22}=E_2/(1-\nu_{12}\nu_{21})$$

$$Q_{12}=\nu_{12}E_1/(1-\nu_{12}\nu_{21})=\nu_{12}E_2/(1-\nu_{12}\nu_{21})$$

$$Q_{66}=G_{12},\quad Q_{16}=Q_{26}=0 \tag{26}$$

Again, if the principal axes 1, 2 are rotated a $+\theta$ from the reference axes x, y, the transformation is the same as that for the compliance parameter in Eqs. (18). The detailed expressions may be obtained by using Eqs. (18) with the replacement of $\bar{S}_{ij}$ and S_{ij} by $\bar{Q}_{ij}$ and Q_{ij}.

It is believed that the presently proposed strain-stress relation for the metallic mesh is unique, because it accommodates both the geometrical nonlinearity and the woven nonlinear behavior of the mesh and because it is not available in the existing literature.

Experiment

The knitted materials that were evaluated have a nonlinear stress-strain relationship. These materials exhibit a very low in-plane stiffness, which results in large deformations. They resist tensile and shear loads, but no compressive loads. Because of these characteristics, which are unusual to structural materials, no standard test procedure is available. It is necessary to develop a test that would be able to accommodate the large deformation with relatively small applied loads.

The approach used to load the test samples is to apply incremental loads to a sample mounted on a flat table (Fig. 3). The table used was 36 in. × 36 in. On the periphery of the table 44 pulleys, 11 per side, are mounted on a horizontal shaft. The pulleys are laterally adjusted to compensate for the deformation of the mesh. The tops of the pulleys are above the surface of the table to eliminate the drag force. To load the knitted mesh, hooks are evenly spaced along the four sides. Lines are attached to the hooks and run over the pulleys, where weights are added or subtracted. Recording of the deformation is accomplished by two methods. First, the overall dimensions are recorded with each load level. Second, a photograph is taken of the material over a one inch square pattern of scribed lines.

Molybdenum and nichrome wire tricot knits were tested. Various wire diameters and numbers of filaments per end were used (Table 1). It was necessary to stretch the material lightly before cutting. The test coupons were cut at 3 different angles with respect to the principal axis of the material: 0, 22.5, and 45 deg.

It was necessary to apply an initial load to eliminate curvature. The same initial load was applied in both directions of a sample. Holding the load constant on the 1-direction, the load was incremented in the 2-direction until a predetermined maximum was reached. Then the load in the 1-direction was incremented and the loading cycle was repeated in the 2-direction. This was continued until the load in both directions reached the maximum. At each load level the overall dimensions were recorded and a photograph taken.

Each coupon was tested three times. After the first test, a permanent set was observed. The stress-strain data of the second and third tests were close. Samples cut coincident with the principal axes of the material remained rectangular (Fig. 4). Samples cut on the bias became skewed and took on the shape of a diamond (Fig. 5).

Comparison of Theory and Experimental Data

Experiments were repeated three times for each loading condition. The first set of data is discarded and the average value of the other two tests is taken as typical of that loading condition. Therefore, the data presented here are for the mesh being prestretched; this is not unreasonable because the actual

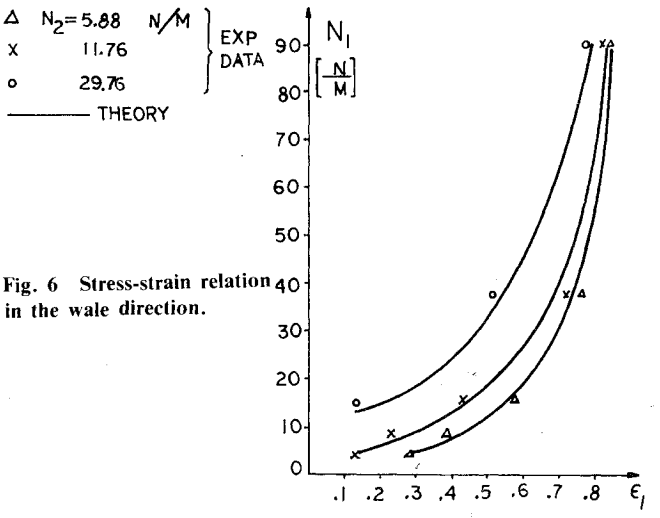

Fig. 6 Stress-strain relation in the wale direction.

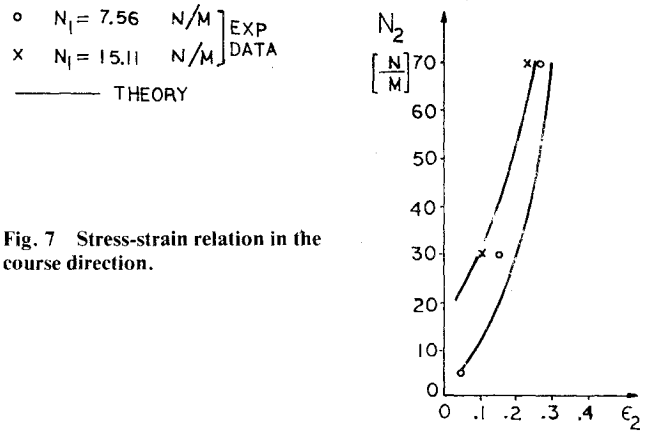

Fig. 7 Stress-strain relation in the course direction.

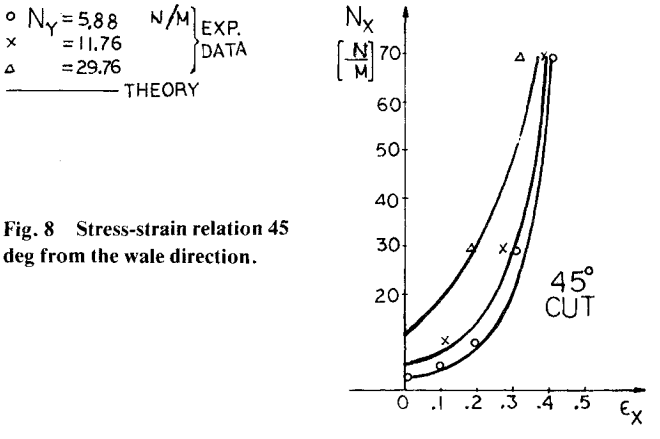

Fig. 8 Stress-strain relation 45 deg from the wale direction.

antenna should be tested, or prestretched, at least once before being sent into space.

The numerical values of the constants in Eqs. (12) are chosen as $n=5$, $K=200$ N/m, $C_1=1$, $C_2=0.45$, and $C_3=0.5$, so that the first of Eqs. (12) fits as closely as possible the N_1-ϵ_1 curve in Fig. 6 with $N_2=5.88$ N/m and the first of Eqs. (16) fits the N_x-ϵ_x relation in Fig. 8 with $N_y=5.88$ N/m. The other curves are predicted with the same data. It can be seen from Figs. 6-8 that the present theory provides a reasonably good description of the stress-strain behavior in the two principal directions as well as for a 45 deg rotation from the principal direction.

The experimental data presented in Figs. 9 and 10 show the result of biaxially loading a mesh specimen with edges cut at a

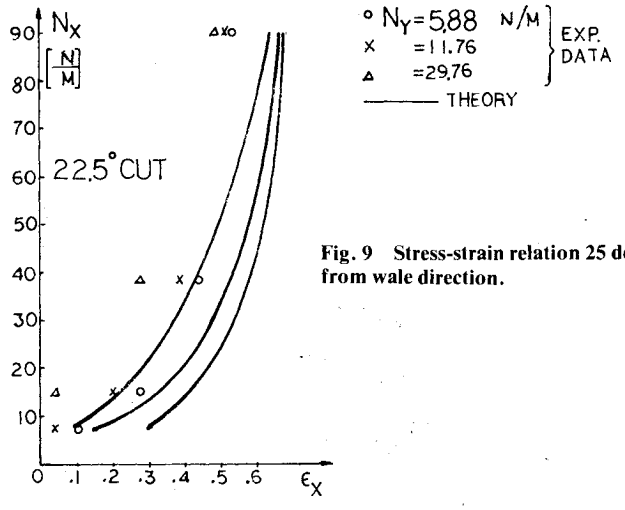

Fig. 9 Stress-strain relation 25 deg from wale direction.

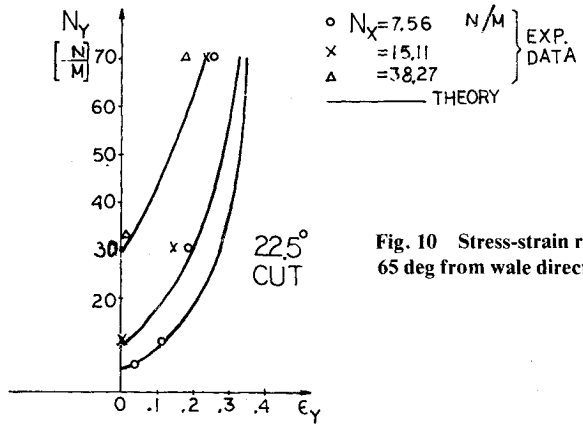

Fig. 10 Stress-strain relation 65 deg from wale direction.

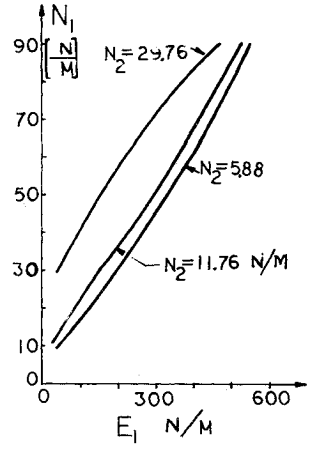

Fig. 11 Effective elastic modulus in wale direction, E_1.

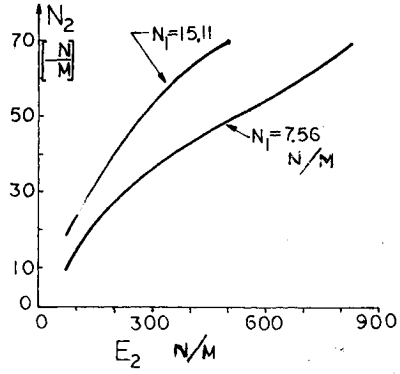

Fig. 12 Effective elastic modulus in course direction, E_2.

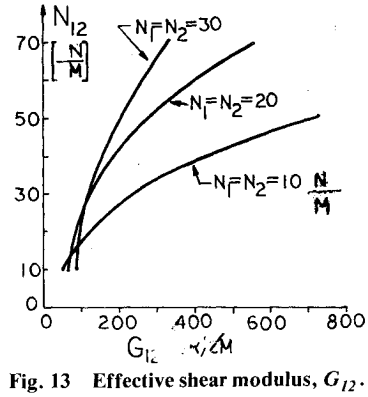

Fig. 13 Effective shear modulus, G_{12}.

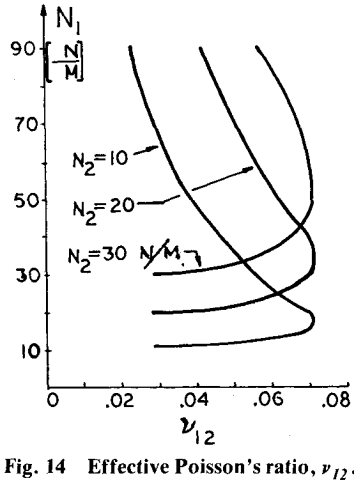

Fig. 14 Effective Poisson's ratio, ν_{12}.

nominal orientation of 22.5 deg with respect to the wale and course material directions. Theoretical results with loads oriented exactly 22.5 deg from the wale direction fell far to the right of the test data. The disagreement may be explained as follows. The initial angular orientation of edge loads with respect to the wale and course directions is a discontinuous step function with respect to cell size for any ratio of biaxial loading. This is a result of the discrete cellular nature of the mesh and the associated finite number of load introduction sites. Thus, in general, the actual angular orientations of applied loads can be quite different from the cut-edge angle.

Recognizing the probability of a test load misalignment of several degrees, we have taken the liberty of plotting theoretical results for a mesh loaded at 25 deg to the wale direction. This shifts the theoretical data to the left, closer to experimental results, yet still preserves the characteristic nonlinear shape.

For most engineering applications, the loading direction is either parallel to or at 45 deg from the wale and course directions. Other angles of alignment are not usually used. Therefore, a satisfactory prediction of the mesh behavior in the wale and course directions as well as in the direction of a 45-deg rotation, should be adequate for practical application.

For design and analysis purposes, it is convenient to know the elastic modulus and Poisson's ratio. Therefore, the effective elastic modulii in the two principal directions E_1 and E_2 are shown in Figs. 11 and 12. These are called "effective" because they represent the global elastic behavior of the mesh instead of the true material property of the metallic yarn. The effective shear modulus G_{12} and the effective Poisson's ratio ν_{12} are shown in Figs. 13 and 14, respectively.

Conclusion

The two-dimensional, orthotropic, nonlinear elastic stress-strain law proposed here seems to give a satisfactory description of the metallic mesh behavior in the two principal directions as well as at a 45 deg rotation from the principal direction. The effective elastic moduli, effective shear modulus, and effective Poisson's ratios defined in this paper should provide engineers with a useful tool for the design and analysis of space antennas made of metallic mesh.

References

[1] Coplan, M. I., Freeston, Jr., W. D., and Platt, M. M., "Flexible Fibrous Structural Material," Fabric Research Lab. Inc., Dedham, Mass., Tech. Doc., Rept. ML-TDR-64-102, Feb. 1964.

[2] Fisher, J. G., "Mesh Materials for Deployable Antennas," *JPL Space Programs Summary 37-65*, Jet Prop. Lab., Pasadena, Calif., Vol. III, Oct. 31, 1970, pp. 122-125.

[3] Levy, D. J. and Momyer, W. R., "Metallic Meshes for Deployable Spacecraft Antennas," Parts I and II, *SAMPE Journal*, Vol. 9, May-June 1973, pp. 4-7; July-Aug. 1973, pp. 12-16.

[4] Morre, D. M., "Lightweight 3.66-Meter-Diameter Conical Mesh Antenna Reflector," Jet Prop. Lab., Pasadena, Calif., JPL Tech. Memo 33-688, June 15, 1974.

[5] "AAFE Large Deployable Antenna Development Program," Harris Corp., Melbourne, Fla., NASA Contract NAS1-13943, Final Rept., 1975.

[6] Popper, P., "The Theoretical Behavior of a Knitted Fabric Subjected to Biaxial Stresses," *Textile Research Journal*, Vol. 36, 1966, pp. 148-157.

[7] Odqvist, F.K.G., *Mathematical Theory of Creep and Creep Rupture*, Oxford Univ. Press, 1966.

[8] Tang, S., "Creep of Laminated Anisotropic Cylindrical Shells," *Hydromechanically Loaded Shells*, edited by R. Szilard, Univ. of Hawaii Press, 1973, pp. 742-752.

[9] Hill, R., *The Mathematical Theory of Plasticity*, Clarendon Press, Oxford, 1950.

[10] Anderson, R. E., "A Variational Theorem for Laminated Composite Plate of Nonlinear Materials and Applications to Post-buckling," Ph.D. Dissertation, Stanford Unv., 1978.

[11] Ashton, J. E., Halpin, J. C., and Petit, P. H., *Primer on Composite Materials: Analysis*, Technomic Publ. Co., Stamford, Conn., 1969.